

Novel Search for absorption of ultra-light fermionic dark matter on electron with cosmic ray boost

X. P. Geng,^{1,*} B. Zhong,¹ and Z. H. Zhang²

¹*Institute of Applied Physics and Computational Mathematics, Beijing 100094, China*

²*Beijing Normal University at Zhuhai, Zhuhai 519087, China*

(Dated: February 24, 2025)

The search for the absorption of fermionic dark matter (DM) on electron is hindered by a partial or complete loss of sensitivity for the mass of DM (m_χ) below $\mathcal{O}(10)$ keV. We introduce a novel search using a small but high-energy portion of DM boosted by cosmic rays, and the loss of sensitivity is circumvented because the subsequent absorption within the detector imparts to the target electron not only m_χ but also substantial T_χ . The one-sided 90% confidence level constraints on $(\sigma_e v_\chi)$ are derived with the XENONnT public dataset for $m_\chi \in (1 \times 10^{-5} - 1)$ keV which has not been explored yet. Our results have placed constraints on DM at the lowest m_χ currently achievable among the DMDD experiments utilizing ionizing signals from DM interactions within the detectors.

Introduction.— A multitude of astronomical and cosmological observations strongly imply the presence of dark matter (DM, denoted as χ), whose enigmatic nature has persisted as one of the most elusive and intriguing scientific challenges for decades [1–5]. Numerous prominent DM candidates, including weakly interacting massive particles [6–12], dark photon DM [13–22], and axion-like particle DM [13, 15, 21, 23–32], have been the focus of vigorous experimental exploration, yet the absence of definitive results has prompted the development of alternative DM models [33–36].

Recently, a newly presented interaction scenario involving the absorption of fermionic dark matter by an electron target ($\chi + e^- \rightarrow \nu + e^-$) has garnered attention and been subjected to investigation within the research community [37–40]. Within this specific scenario, the absorption of dark matter is accompanied by the emission of an outgoing neutrino, and the target electron can acquire kinetic energy from both the mass of DM (m_χ) and the kinetic energy of DM (T_χ). The DM detectors can register the corresponding energy deposited, providing an opportunity to search for this scenario in the dark matter direct detection (DMDD).

In previous studies of the scenario, the Standard Halo Model (SHM) [41, 42] is adopted, wherein DM possessing a typical velocity $v_\chi \sim 10^{-3}c$ results in a negligible T_χ compared to m_χ [37–40]. The latest results from PandaX-4T [37] have reached a detection lower limit of $m_\chi = 10$ keV and its “optimal” m_χ region lies on $m_\chi \in (40\text{--}100)$ keV with corresponding $(\sigma_e v_\chi) < 1 \times 10^{-49} \text{cm}^2$ for axial-vector interaction. While below the “optimal” m_χ region, the direct detection sensitivity to DM diminishes swiftly due to the reduction in electronic recoil energy which cannot exceed m_χ . Furthermore, if m_χ falls below the detection threshold, the detector will completely lose its capability to detect this scenario.

Fortunately, it has come to light that numerous processes can accelerate a subdominant component of DM to a much higher T_χ . Primary potential avenues include:

(1) DM particles collide with high-energy Galactic cosmic rays (CR) [43–46]. (2) DM particles engage in scattering interactions with rapidly moving nuclei or electrons inside the Sun (solar reflection) [47–49]. (3) DM particles from the evaporation of Primordial Black Holes can possess higher energy [50, 51].

We consider a secondary yet inevitably present fraction of the DM flux where DM receives an impetus from the aforementioned CR and subsequently attains a significantly elevated T_χ , this specific part of DM is referred to as CRDM. The CRDM will go through the aforementioned absorption process with both m_χ and notable T_χ , leading to a heightened deposited energy registered in the detector. As a consequence, the detectable range of the m_χ can be extended into the ultra-light region, enabling the exploration of previously inaccessible areas of DM parameter space (theoretically extending to $m_\chi \rightarrow 0$).

In this letter, leveraging the kinetic enhancement provided by CR, we employ the electronic recoil data from XENONnT [52] which is one of the most state-of-the-art DMDD experiments, to perform a search for the absorption of ultra-light fermionic DM on electron, and the constraints of this scenario are derived with $m_\chi \in (1 \times 10^{-5} - 1)$ keV. The boost of DM from CR is presumed to occur via spin-independent (SI) scattering in this work, this assumption is made as the paper does not intend to delve into the mechanisms underlying the production of CRDM.

CRDM flux.— CRs in the vicinity of Earth, which are assumed to originate from supernova remnants, are high-energy particles consisting of protons, electrons, and an assortment of heavier nuclei such as ^4He [53, 54]. Electrically charged CRs interact with Galactic magnetic fields during their propagation. These interactions cause the CR trajectories to undergo numerous scatterings due to the irregular and turbulent nature of the magnetic fields. This process effectively randomizes their original directions, leading to the isotropic distribution observed on Earth [55]. The Local Interstellar Spectra (LIS) of CR

proton and ${}^4\text{He}$, the two primary components, can be evaluated by Eq. 1.

$$\frac{dI}{dR} \times R^{2.7} = \begin{cases} \sum_{i=0}^5 a_i R^i, & R \leq 1 \text{ GV} \\ b + \frac{c}{R} + \frac{d_1}{d_2 + R} + \frac{e_1}{e_2 + R} \\ + \frac{f_1}{f_2 + R} + gR, & R > 1 \text{ GV} \end{cases} \quad (1)$$

where R is the magnetic rigidity of the specific particle, the rest parameters are listed in Table. I.

TABLE I. The efficiencies in Eq. 1 describing the differential intensities of CR proton and ${}^4\text{He}$ [56, 57].

	a_0	a_1	a_2	a_3	a_4	a_5	b	c
p	94.1	-831	0	16700	-10200	0	10800	8500
${}^4\text{He}$	1.14	0	-118	578	0	-87	3120	-5530
	d_1	d_2	e_1	e_2	f_1	f_2	g	
p	-4230000	3190	274000	17.4	-39400	0.464	0	
${}^4\text{He}$	3370	1.29	134000	88.5	-1170000	861	0.03	

The LIS of CR flux as a function of kinetic energy T is expressed by $\frac{d\Phi^{\text{LIS}}}{dT} = 4\pi \frac{dI}{dR} \frac{dR}{dT}$, where $\frac{dR}{dT}$ should be calculated with account for relativity shown in Eq. 2.

$$\frac{dR}{dT} = \frac{1}{Q} \frac{T + m_i}{T^2 + 2Tm_i}, \quad (2)$$

where Q is the electric charge of CR particle i , m_i is the mass of CR particle i .

DM particles can be considered at rest compared to CR particles traveling at relativistic velocities. The kinetic energy transferred to a DM particle T_χ from the CR particle in a single collision is described in Eq. 3.

$$T_\chi = T_\chi^{\text{max}} \frac{1 - \cos \theta_s}{2},$$

$$T_\chi^{\text{max}} = \frac{T_i^2 + 2m_i T_i}{T_i + (m_i + m_\chi)^2 / (2m_\chi)}, \quad (3)$$

where T_i is the kinetic energy of the incident CR particle i , m_χ is the mass of DM, θ_s is the scattering angle between DM and CR particle i in the center-of-mass reference frame. Conversely, the minimum kinetic energy of the CR particle required to impart a DM kinetic energy of T_χ is given by Eq. 4.

$$T_i^{\text{min}} = \left(\frac{T_\chi}{2} - m_i \right) \left(1 \pm \sqrt{1 + \frac{2T_\chi (m_i + m_\chi)^2}{m_\chi (2m_i - T_\chi)^2}} \right), \quad (4)$$

where $+$ ($-$) corresponds to $T_\chi > 2m_i$ ($T_\chi < 2m_i$).

The differential CRDM flux is derived by Eq. 5, with integration over all the CR proton and ${}^4\text{He}$ along the Line of Sight (LOS).

$$\frac{d\Phi_\chi}{dT_\chi} = \sum_i \int \frac{d\Omega}{4\pi} \int_{\text{LOS}} dl \int_{T_i^{\text{min}}}^{\infty} \frac{\rho_\chi(r)}{m_\chi} \frac{d\sigma_{\chi i}}{dT_\chi} \frac{d\Phi_i(r)}{dT_i} dT_i, \quad (5)$$

where Ω is the solid angle, $\rho_\chi(r)$ is the DM density distribution which the Navarro-Frenk-White (NFW) profile [58, 59] is adopted, $\frac{d\Phi_i(r)}{dT_i}$ is the CR flux spatial distribution of the CR particle i , treated as homogeneous in this work [43]. The differential cross-section of DM and CR particle $\frac{d\sigma_{\chi i}}{dT_\chi}$ is shown in Eq. 6

$$\frac{d\sigma_{\chi i}}{dT_\chi} = \frac{\sigma_{\chi N}^{\text{SI}}}{T_\chi^{\text{max}}} A_i^2 \left(\frac{\mu_{\chi i}}{\mu_{\chi N}} \right)^2 G_i^2(Q^2), \quad (6)$$

where $\sigma_{\chi N}^{\text{SI}}$ is the zero-momentum transferred DM-nucleon cross section for SI scattering, A_i is the mass number of CR particle i , $\mu_{\chi i}$ and $\mu_{\chi N}$ are the reduced masses of DM- i and DM-nucleon, respectively. $G(Q^2)$ is the form factor with $Q^2 = 2m_\chi T_\chi$, for proton and ${}^4\text{He}$, the dipole form factor $G_i(Q^2) = 1/(1 + Q^2/\Lambda_i^2)^2$ is adopted, where $\Lambda_p \simeq 770$ MeV and $\Lambda_{{}^4\text{He}} \simeq 410$ MeV [60].

Combining the related items above, we can obtain $\frac{d\Phi_\chi}{dT_\chi}$ shown in Eq. 7.

$$\frac{d\Phi_\chi}{dT_\chi} = D_{\text{eff}} \frac{\rho_\chi^{\text{local}}}{m_\chi} \times \sum_i \sigma_{\chi N}^{\text{SI}} A_i^2 \left(\frac{\mu_{\chi i}}{\mu_{\chi N}} \right)^2 G_i^2(2m_\chi T_\chi) \int_{T_i^{\text{min}}}^{\infty} dT_i \frac{d\Phi_i^{\text{LIS}}/dT_i}{T_\chi^{\text{max}}(T_i)}, \quad (7)$$

where $\rho_\chi^{\text{local}} \sim 0.3$ GeV/cm³ is the local density of DM, D_{eff} is the spatial extent effectively contributing to CR and DM interactions, dependent on their distributions in the Milky Way. With the NFW profile for the DM distribution and the homogeneous CR spatial distribution, $D_{\text{eff}} = \int \frac{d\Omega}{4\pi} \int_{\text{LOS}} \frac{\rho_\chi(r)}{\rho_\chi^{\text{local}}} dl$, the LOS is set to 1 kpc to obtain a conservative result, yielding $D_{\text{eff}} = 0.997$ kpc in this work. The CRDM fluxes for various m_χ are shown in Fig. 1, with the DM fluxes under the SHM for comparison.

Signal model.— The fermionic CRDM-electron absorption can be induced by vector (V) and axial-vector (A) operators [38] shown in Eq. 8

$$\mathcal{O}_{e\nu\chi}^V = \frac{1}{\Lambda^2} (\bar{e}\gamma_\mu e)(\bar{\nu}_L\gamma^\mu\chi_L),$$

$$\mathcal{O}_{e\nu\chi}^A = \frac{1}{\Lambda^2} (\bar{e}\gamma_\mu\gamma_5 e)(\bar{\nu}_L\gamma^\mu\chi_L), \quad (8)$$

where the Standard Model neutrino is taken, $1/\Lambda^2$ is the Wilson coefficient with a dimension of (mass)⁻².

Momentum conservation gives Eq. 9 describing the outgoing momentum of the neutrino.

$$p_\nu = |p_\chi - q| = \sqrt{p_\chi^2 + q^2 - 2m_\chi v_\chi q \cos \theta_{p_\chi q}}, \quad (9)$$

where p_χ is the momentum of the DM particle, q is the momentum transferred to the target electron, $\theta_{p_\chi q}$ is the

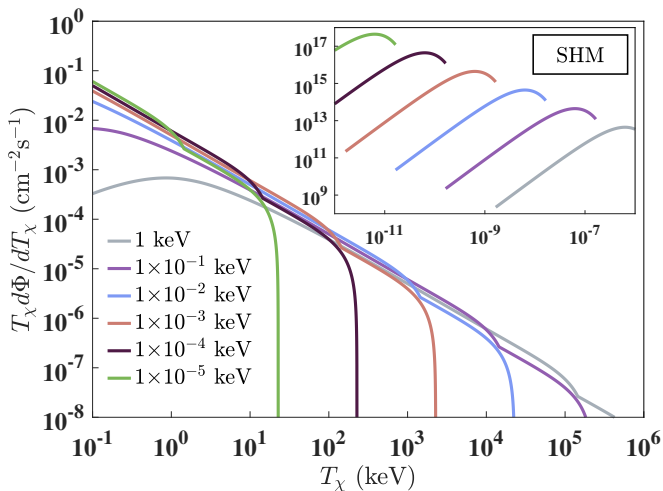


FIG. 1. CRDM fluxes for various m_χ with $\sigma_{\chi N}^{\text{SI}} = 10^{-31} \text{ cm}^2$ and $D_{\text{eff}} = 0.997 \text{ kpc}$. Inset: The DM fluxes under the SHM for the same m_χ , the axes of the inset are identical to those of the main figure.

angle between p_χ and q under the lab frame. In combination with the minuscule mass of the active neutrino [61], we can obtain Eq. 10 via energy conservation.

$$m_\chi + T_\chi - \sqrt{p_\chi^2 + q^2 - 2p_\chi q \theta_{p_\chi q}} = |E_B^{nl}| + E_R, \quad (10)$$

where E_R is the recoil energy, $|E_B^{nl}|$ is the binding energy of the atomic electron with quantum number (n, l) [62]. The deposited energy in the detector E_{det} comprises both the binding energy and the recoil energy, $E_{\text{det}} = |E_B^{nl}| + E_R$. Correspondingly, q is derived in Eq. 11.

$$q = p_\chi \cos \theta_{p_\chi q} \pm \sqrt{p_\chi^2 (\cos^2 \theta_{p_\chi q} - 1) + (T_\chi + m_\chi - E_{\text{det}})^2}, \quad (11)$$

where $+$ ($-$) corresponds to $\cos \theta_{p_\chi q} \leq 0$ ($\cos \theta_{p_\chi q} > 0$).

The expected differential event rate of fermionic DM-electron absorption is shown in Eq. 12.

$$\begin{aligned} \frac{dR}{dE_{\text{det}}} &= N_T \sum_{nl} \int v_\chi \frac{d\Phi_\chi}{dT_\chi} \frac{q}{64\pi m_e^2 m_\chi (E_{\text{det}} - |E_B^{nl}|)} \\ &\times |M(q)|^2 |f_{\text{ion}}^{nl}(k', q)|^2 dT_\chi, \end{aligned} \quad (12)$$

where N_T is the number of targets per unit mass with all (n, l) shell bound electrons included, m_e is the electron mass, $|f_{\text{ion}}^{nl}(k', q)|^2$ with $k' = \sqrt{(E_{\text{det}} - |E_B^{nl}| + m_e)^2 - m_e^2}$ is the ionization form factor calculated by *DarkART* [63, 64]. $|M(q)|^2$ is the scattering matrix element shown in Eq. 13 with different operators.

$$|M^{(V, A)}(q)|^2 = (1, 3) \times \frac{16\pi m_e^2 q}{m_\chi} (\sigma_e v_\chi), \quad (13)$$

where σ_e is the cross section of free electron-DM scattering and can be formulated as $\sigma_e \equiv (m_\chi^2 / 4\pi v_\chi \Lambda^4)$.

The expected event rates of fermionic CRDM-electron absorption induced by V operator in the XENONnT detector with $m_\chi = 1 / 1 \times 10^{-5} \text{ keV}$ are shown in Fig. 2 as an example, along with the XENONnT electronic recoil data.

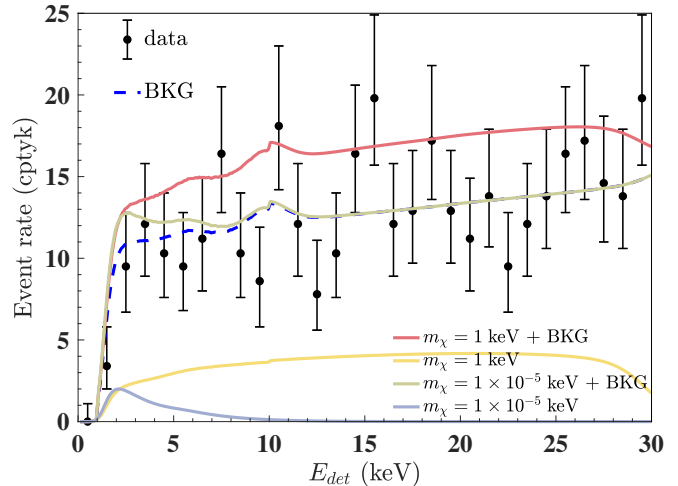


FIG. 2. Expected event rates of fermionic CRDM-electron absorption for $(m_\chi, \sigma_e v_\chi) = (1 \text{ keV}, 2 \times 10^{-33} \text{ cm}^2)$ and $(1 \times 10^{-5} \text{ keV}, 2 \times 10^{-41} \text{ cm}^2)$, with $D_{\text{eff}} = 0.997 \text{ kpc}$ and $\sigma_{\chi N}^{\text{SI}} = 10^{-31} \text{ cm}^2$. The electronic recoil data from XENONnT public dataset is plotted as points with error bars, the blue line represents XENONnT background model (BKG) extracted from Ref. [65].

Exclusion result.— We apply the minimum- χ^2 analysis in this work, where the χ^2 is defined in Eq. 14.

$$\chi^2 = \sum_i \frac{[n_i - (S_i + B_i)]^2}{\Delta_i^2}, \quad (14)$$

where n_i is the measured count rate in the detector at the i -th energy bin, Δ_i is the uncertainty at the i -th energy bin with both the statistical and systematic components, S_i is the expected count rate within the signal model at the i -th energy bin, and B_i is the background model of XENONnT [65] at the i -th energy bin.

With the XENONnT public dataset, no significant signal is observed. The one-sided 90% confidence level (CL) constraints on $(\sigma_e v_\chi)$ with both V and A operators for $m_\chi \in (1 \times 10^{-5} - 1) \text{ keV}$ are obtained, adequately encompassed by the XENONnT dataset. The results are shown in Fig. 3. The numerical value of the constraints on $(\sigma_e v_\chi)$ is inversely proportional to $\sigma_{\chi N}^{\text{SI}}$ at corresponding m_χ . Owing to the absence of experimental constraints on $\sigma_{\chi N}^{\text{SI}}$ for $m_\chi \in (1 \times 10^{-5} - 1) \text{ keV}$, the $\sigma_{\chi N}^{\text{SI}}$ is set to $1 \times 10^{-31} \text{ cm}^2$ from a previous study on CRDM [43] for a conservative evaluation. Nevertheless, this does not affect the span of m_χ for which the constraints can be derived.

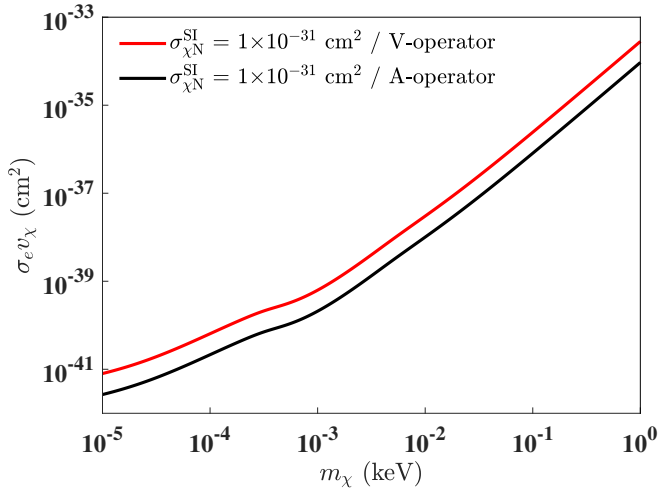


FIG. 3. One-sided 90% CL constraint on $(\sigma_e v_\chi)$ for the V operator and A operator imposed by the XENONnT experiment with different $\sigma_{\chi N}^{\text{SI}}$.

Our results exclude the fermionic DM-electron absorption cross section $(\sigma_e v_\chi)$ mediated by V (A) operator from 8.0×10^{-42} (2.7×10^{-42}) – 2.8×10^{-34} (9.3×10^{-35}) cm^2 for $m_\chi \in (1 \times 10^{-5} - 1)$ keV. This particular region remains unexplored in previous studies and our results reach the lowest m_χ to date among the DMDD experiments utilizing the ionizing signals from DM interactions within the detectors.

Conclusion.— We demonstrate that the subdominant while energetic component of DM boosted by CR can impose a novel constraint on $(\sigma_e v_\chi)$ for a range of m_χ which was previously deemed inaccessible.

In this work, we explored the parameter space on $(m_\chi, \sigma_e v_\chi)$ of ultra-light fermionic DM-electron absorption induced by V and A operators with the consideration of boost from CR for the first time. Employing the 1.16 tonne-year XENONnT public dataset, the one-sided 90% CL constraints on $(\sigma_e v_\chi)$ for $m_\chi \in (1 \times 10^{-5} - 1)$ keV are derived. Constraints have been derived on DM at the smallest m_χ currently accessible among DMDD experiments using ionizing signals from DM interactions within detectors.

* Corresponding author: gxp18@tsinghua.org.cn

- [1] A. Cho, *Science* **339**, 1513 (2013).
- [2] A. Arbey and F. Mahmoudi, *Prog. Part. Nucl. Phys.* **119**, 103865 (2021).
- [3] G. Bertone and T. M. P. Tait, *Nature* **562**, 51 (2018).
- [4] J. Liu, X. Chen, and X. Ji, *Nat. Phys.* **13**, 212 (2017).
- [5] S. Cebrián, *J. Phys. Conf. Ser.* **2502**, 012004 (2023).
- [6] E. Aprile, *et al.* (XENON Collaboration), *Phys. Rev. Lett.* **131**, 041003 (2023).
- [7] R. Agnese, *et al.* (SuperCDMS Collaboration),

- Phys. Rev. Lett.* **120**, 061802 (2018).
- [8] J. Aalbers, *et al.* (LUX-ZEPLIN Collaboration), *Phys. Rev. Lett.* **131**, 041002 (2023).
- [9] Z. Bo, *et al.* (PandaX Collaboration), *Phys. Rev. Lett.* **134**, 011805 (2025).
- [10] P. Agnes, *et al.* (DarkSide Collaboration), *Phys. Rev. Lett.* **121**, 081307 (2018).
- [11] P. Adari, *et al.* (SENSEI Collaboration), *Phys. Rev. Lett.* **134**, 011804 (2025).
- [12] H. Jiang, *et al.* (CDEX Collaboration), *Phys. Rev. Lett.* **120**, 241301 (2018).
- [13] E. Aprile, *et al.* (XENON Collaboration), *Phys. Rev. Lett.* **129**, 161805 (2022).
- [14] E. Aprile *et al.* (XENON Collaboration), *Phys. Rev. D* **102**, 072004 (2020).
- [15] E. Aprile, *et al.* (XENON Collaboration), *Phys. Rev. Lett.* **123**, 251801 (2019).
- [16] Z. Tang, *et al.* (SHANHE Collaboration), *Phys. Rev. Lett.* **133**, 021005 (2024).
- [17] Z. She, *et al.* (CDEX Collaboration), *Phys. Rev. Lett.* **124**, 111301 (2020).
- [18] X. P. Geng, *et al.* (CDEX Collaboration), *Phys. Rev. D* **107**, 112002 (2023).
- [19] A. Aguilar-Arevalo, *et al.* (DAMIC Collaboration), *Phys. Rev. Lett.* **123**, 181802 (2019).
- [20] T. Aralis, *et al.* (SuperCDMS Collaboration), *Phys. Rev. D* **101**, 052008 (2020).
- [21] K. Abe, *et al.*, *Phys. Lett. B* **787**, 153 (2018).
- [22] S. Bilmiş, *et al.*, *Phys. Rev. D* **92**, 033009 (2015).
- [23] V. Anastassopoulos, *et al.* (CAST Collaboration), *Nat. Phys.* **13**, 584 (2017).
- [24] C. M. Adair, *et al.*, *Nat. Commun.* **13**, 6180 (2022).
- [25] M. Jiang, *et al.*, *Nat. Phys.* **17**, 1402 (2021).
- [26] A. V. Gramolin, *et al.*, *Nat. Phys.* **17**, 79 (2021).
- [27] D. S. Akerib, *et al.* (LUX Collaboration), *Phys. Rev. Lett.* **118**, 261301 (2017).
- [28] E. Armengaud, *et al.* (EDELWEISS Collaboration), *Phys. Rev. D* **98**, 082004 (2018).
- [29] Y. Wang, *et al.* (CDEX Collaboration), *Phys. Rev. D* **101**, 052003 (2020).
- [30] N. Abgrall, *et al.* (Majorana Collaboration), *Phys. Rev. Lett.* **118**, 161801 (2017).
- [31] C. Fu, *et al.* (PandaX Collaboration), *Phys. Rev. Lett.* **119**, 181806 (2017).
- [32] T. Aralis, *et al.* (SuperCDMS Collaboration), *Phys. Rev. D* **101**, 052008 (2020).
- [33] C. Kouvaris and J. Pradler, *Phys. Rev. Lett.* **118**, 031803 (2017).
- [34] G. G. di Cortona, A. Messina, and S. Piacentini, *J. High Energy Phys.* **2020**, 34 (2020).
- [35] Y. Hochberg, *et al.*, *Phys. Rev. Lett.* **128**, 191801 (2022).
- [36] M. Ibe, *et al.*, *J. High Energy Phys.* **2018**, 194 (2018).
- [37] D. Zhang, *et al.* (PandaX Collaboration), *Phys. Rev. Lett.* **129**, 161804 (2022).
- [38] J. A. Dror, *et al.*, *Phys. Rev. D* **103**, 035001 (2021).
- [39] S.-F. Ge, *et al.*, *J. High Energy Phys.* **2022**, 191 (2022).
- [40] J. X. Liu *et al.* (CDEX Collaboration), arXiv:2404.09793 (2024).
- [41] A. K. Drukier, K. Freese, and D. N. Spergel, *Phys. Rev. D* **33**, 3495 (1986).
- [42] G. Jungman, M. Kamionkowski, and K. Griest, *Phys. Rep.* **267**, 195 (1996).
- [43] T. Bringmann and M. Pospelov, *Phys. Rev. Lett.* **122**, 171801 (2019).

- [44] X. Shang, *et al.* (PandaX Collaboration), Phys. Rev. Lett. **133**, 101805 (2024).
- [45] R. Xu, *et al.* (CDEX Collaboration), Phys. Rev. D **106**, 052008 (2022).
- [46] G. Guo, Y.-L. S. Tsai, and M.-R. Wu, J. Cosmol. Astropart. Phys. **2020**, 049 (2020).
- [47] H. An, *et al.*, Phys. Rev. Lett. **120**, 141801 (2018).
- [48] H. An, *et al.*, Phys. Rev. D **104**, 103026 (2021).
- [49] Z. Y. Zhang, *et al.* (CDEX Collaboration), Phys. Rev. Lett. **132**, 171001 (2024).
- [50] R. Calabrese, *et al.*, Phys. Rev. D **105**, L021302 (2022).
- [51] Z. H. Zhang, *et al.* (CDEX Collaboration), Phys. Rev. D **108**, 052006 (2023).
- [52] E. Aprile *et al.* (XENON Collaboration), Eur. Phys. J. C **84**, 261001 (2024).
- [53] C. J. Cesarsky, Annu. Rev. Astron. Astrophys. **18**, 289 (1980)
- [54] A. M. Bykov, *et al.*, Space Sci. Rev. **214**, 41 (2018).
- [55] A. W. Strong, I. V. Moskalenko, and V. S. Ptuskin, Annu. Rev. Nucl. Part. Sci. **57**, 285 (2007).
- [56] M. J. Boschini, *et al.*, Astrophys. J. **840**, 115 (2017).
- [57] M. J. Boschini, *et al.*, Astrophys. J. **858**, 61 (2018).
- [58] J. F. Navarro, C. S. Frenk, and S. D. M. White, Astrophys. J. **462**, 563 (1996).
- [59] M. Ackermann, *et al.*, Astrophys. J. **761**, 91 (2012).
- [60] C. Perdrisat, V. Punjabi, and M. Vanderhaeghen, Prog. Part. Nucl. Phys. **59**, 694 (2007).
- [61] M. Aker, *et al.* (KATRIN Collaboration), Nat. Phys. **18**, 160 (2022).
- [62] C. Bunge, J. Barrientos, and A. Bunge, At. Data Nucl. Data Tables **53**, 113 (1993).
- [63] R. Catena, *et al.*, Phys. Rev. Res. **2**, 033195 (2020).
- [64] T. Emken, “Dark Atomic Response Tabulator (DarkART)[Code, v0.1]”, code can be found under <https://github.com/temken/darkart>. (2021).
- [65] E. Aprile *et al.* (XENON Collaboration), Phys. Rev. Lett. **129**, 161805 (2022).